

# **Archive ouverte UNIGE**

https://archive-ouverte.unige.ch

Article scientifique

Article

1985

**Published version** 

**Open Access** 

This is the published version of the publication, made available in accordance with the publisher's policy.

Raman spectroscopic study of structural phase transitions in the layer crystals (EtNH3)2MCl4 with M=Cd and Mn

Hagemann, Hans-Rudolf; Bill, Hans

# How to cite

HAGEMANN, Hans-Rudolf, BILL, Hans. Raman spectroscopic study of structural phase transitions in the layer crystals (EtNH3)2MCl4 with M=Cd and Mn. In: Journal of physics. C. Solid state physics, 1985, vol. 18, n° 35, p. 6441–6456. doi: 10.1088/0022-3719/18/35/009

This publication URL: <a href="https://archive-ouverte.unige.ch/unige:3104">https://archive-ouverte.unige.ch/unige:3104</a>

Publication DOI: <u>10.1088/0022-3719/18/35/009</u>

© This document is protected by copyright. Please refer to copyright holder(s) for terms of use.

# Raman spectroscopic study of structural phase transitions in the layer crystals $(EtNH_3)_2MCl_4$ with M = Cd and Mn

## H Hagemann† and H Bill

Groupe de Physico-Chimie du Solide, Université de Genève, 30, quai E Ansermet, 1211 Geneva 4, Switzerland

Received 22 March 1985

**Abstract.** We have studied the Raman spectra of the crystals (EtNH<sub>3</sub>)<sub>2</sub>MCl<sub>4</sub> (M = Cd and Mn) as functions of temperature from 5 to 300 K. The external vibrations have been assigned. The space group of the Cd crystal below 114 K is found to be  $P2_1/b$  and the phase transition  $P2_1/b$ -Pbca is described as a displacive first-order transition. The order-disorder transitions Pbca-Abma in (EtNH<sub>3</sub>)<sub>2</sub>MCl<sub>4</sub> for M = Cd and M = Mn are compared. Linewidth measurements performed on the carbon-carbon stretching mode at about 870 cm<sup>-1</sup> suggest the possibility of a second-order transition in the Mn crystal, while the first-order behaviour of the transition in the Cd crystal is confirmed.

#### 1. Introduction

The layer crystals  $(EtNH_3)_2CdCl_4$  (=EACdC) and  $(EtNH_3)_2MnCl_4$  (=EAMnC) belong to a family of compounds that exhibit structural phase transitions (Kind 1980) triggered by the degrees of freedom of motion of the alkylammonium group. Several transitions encountered in these crystals are order–disorder transitions.

The structural phase transitions of EAMnC and EACdC have been studied by NMR (Blinc et al 1977), crystallographic (Chapuis 1977, Depmeier 1977, Depmeier and Heger 1978), optical (Brunskill and Depmeier 1982, Käräjämäki et al 1981), dielectric (Levstik and Filipic 1980, Filipic and Levstik 1980), calorimetric (Tello et al 1977) and infrared (Oxton 1979, Peyrard and Perret 1979) measurements. They are summarised in table 1. As Raman spectroscopy can give useful complementary information, we have performed a detailed study using this method of EACdC and EAMnC, varying the temperature from 4.2 to 300 K (Hagemann 1984). In the first stage we obtained the Raman spectra of EACdC and two isotopic analogues at very low temperatures (Hagemann and Bill 1982a), and we subsequently discussed qualitatively the phase transitions in EACdC (Hagemann and Bill 1982b).

In the course of our investigations, we became aware of two independent Raman studies, one on EAMnC (Rehaber 1976) and one on EACdC (Mokhlisse *et al* 1982, Mokhlisse 1983). The study on EAMnC (Rehaber 1976) refers mainly to one plane of polarisation in the temperature range from 33 to 440 K. Mokhlisse (1983) has investigated the low-frequency spectra of EACdC in the three crystal phases at room tem-

<sup>†</sup> Present address: Department of Chemistry, University of California, Berkeley, CA 94720, USA.

EAMnC		EACdC
$T_c = 424 \text{ K}$ $\Delta H = 71 \text{ J mol}^{-1}$ $\Delta S = 0.17 \text{ J mol}^{-1} \text{ K}^{-1}$	THT I4/mmm	$T_c = 485 \text{ K}$ $\Delta H = 108 \text{ J mol}^{-1}$ $\Delta S = 0.2 \text{ J mol}^{-1} \text{ K}^{-1}$
a = 735.5  pm b = 726.0  pm c = 2210  pm	ORT Abma	a = 756.5  pm b = 746.4  pm c = 2187.9  pm
$T_c = 226 \text{ K}$ $\Delta H = 762 \text{ J mol}^{-1}$ $\Delta S = 3.5 \text{ J mol}^{-1} \text{ K}^{-1}$		$T_c = 216 \text{ K}$ $\Delta H = 2163 \text{ J mol}^{-1}$ $\Delta S = 9.7 \text{ J mol}^{-1} \text{ K}^{-1}$
a = 732.5  pm b = 715.1  pm c = 2203.5  pm	OLT P <i>bca</i>	a = 747.8  pm b = 735.4  pm c = 2211  pm
	MLT	$T_{\rm c} = 114~{\rm K}$

Table 1. Structural phase transitions in EAMnC and EACdC.

perature and below, and has proposed the assignment of the external modes by comparison with the results obtained on the analogue crystal  $(CH_3NH_3)_2CdCl_4$  (=MACdC) (Mokhlisse *et al* 1983a, b).

The aim of the present paper is to provide additional information on EACdC and EAMnC, which has been obtained through isotopic substitution on the ethylammonium group in EACdC, temperature dependence measurements of Raman linewidth and by an investigation of the Raman spectra of EtNH<sub>3</sub>Cl (Hagemann and Bill 1984). This information yields the following result:

- (i) additional information on the structural phase transitions;
- (ii) the establishment of the space group of EACdC below 114 K;
- (iii) a more confident assignment of the external vibrations at the centre of the Brillouin zone.

### 2. Experimental details

We have prepared the following crystals by slow evaporation in  $H_2O$  and  $D_2O$ : EAMnC, EACdC,  $(nPrNH_3)_2MnCl_4$  (=PAMnC),  $(nPrNH_3)_2CdCl_4$  (=PACdC),  $(CD_3CH_2NH_3)_2CdCl_4$  (=EACdC-d<sub>3</sub>[I]) and  $(EtND_3)_2CdCl_4$  (=EACdC-d<sub>3</sub>[II]). The crystals frequently showed twinning and to ensure that the best quality crystals were used in the experiments, we selected the best specimens using a polarising microscope. Typically, the dimensions of the single crystals were less than  $6 \times 7 \times 2$  mm<sup>3</sup>.

In order to compare our results for the crystals EAMnC and EACdC, we had to choose a common setting of the crystal axes. Geick and Strobel (1977) have performed a group theoretical analysis of the lattice vibrations in these crystals using the setting Abma for EAMnC. We decided to keep this convention and thus the lattice parameters of EACdC at room temperature are a = 7.565 Å, b = 7.464 Å and c = 21.879 Å, while those for EAMnC are a = 7.355 Å, b = 7.260 Å and c = 22.100 Å.

The crystals were studied in a laboratory-assembled Raman spectrometer consisting of the following parts: a Spectra Physics argon-ion laser, a Spex 1403 double monochromator and a Brookdeal photon counting system. The measurements were performed using either the 488 or the 514.5 nm argon laser line with a nominal output power ranging from 0.1 to 0.4 W.

The samples were studied using an Oxford Instruments helium-flow cryostat completed by a temperature controller that measures and displays the temperature through a thermocouple  $Au + 0.02 \, \text{Fe/constantan}$ . This instrument maintains the temperature stable within  $0.1 \, \text{K}$ . The absolute temperature of the sample has been evaluated for EACdC by using the Stokes-anti-Stokes intensity ratio and found to be within  $2 \, \text{K}$  of the displayed temperature. All the temperatures referred to in the following are those read on this temperature controller.

## 3. The crystal symmetry of EACdC below 114 K

We have obtained the low-frequency Raman spectra of EACdC, EACdC-d<sub>3</sub>[I] and EACdC-d<sub>3</sub>[II] at low temperatures (Hagemann and Bill 1982a). The results can be summarised as follows.

- (i) We observe 20 external modes, which may be divided into two groups: 12 modes corresponding to the Raman tensor elements (expressed in the Porto notation) (aa), (bb), (cc) and (bc) and 8 modes corresponding to the elements (ab) and (ac).
- (ii) Polarisation measurements reveal that the spectra related to the tensor elements (ab) and (ba) are identical, while those related to the tensor elements (bc) and (cb) are not.

This anisotropy of the Raman tensor cannot be related to a resonant Raman effect, as the crystal EACdC is transparent between 250 and 1000 nm.

These observations confirm that the crystal undergoes a structural phase transition at 114 K and they lead us to postulate a monoclinic crystal symmetry. An additional argument in favour of this statement can be found by comparing our observed Raman frequencies with the FIR data obtained by Stoelinga and Wyder (1974). There are only very few coincidences between the FIR and Raman frequencies, thus confirming the presence of a centre of inversion in the crystal.

Considering the known orthorhombic crystal structures (Chapuis 1977) of EACdC (space groups Abma and Pbca), we can extrapolate through qualitative arguments to the monoclinic space group  $P2_1/b$  for EACdC below 114 K. This is also the space group of MACdC below 163 K.

The factor group analysis related to the space group  $P2_1/b$  yields the following result: at the centre of the Brillouin zone, we expect 12 external modes transforming as  $A_g$  and 12 transforming as  $B_g$ . In our system, the Raman tensor elements (aa), (bb), (cc) and (bc) transform as  $A_g$  and the elements (ab) and (ac) transform as  $B_g$ . This group theoretical prediction is in agreement with our experimental observation. Additional information can be obtained through the correlation table (table 2) of the irreducible representations in the three crystal phases of EACdC encountered between 5 and 300 K. The observed changes in the spectra of EACdC in the (bc) plane around the phase transition OLT-MLT (Hagemann and Bill 1982b) can very well be accounted for by this correlation diagram.

Mokhlisse et al (1983a) have recently published the Raman spectra of MACdC in its

**Table 2.** The correlation table of the symmetry of the external modes in the crystals EAMC (M = Mn and Cd) according to Geick and Strobel (1977). N indicates the number of external modes of the corresponding symmetry predicted by factor group analysis.

Abma	Pbca	$P2_1/b$	N
${\Gamma_1^{-}(A_g)}$	Γ <sub>1</sub> (A <sub>g</sub> )	Γ <sub>1</sub> (A <sub>e</sub> )	6
$Z_4^-(A_g)$ —	$\Gamma_1^ (A_g)$ $\longrightarrow$	$ Z_1^-(A_g)$	6
	Γ <sub>4</sub> (B <sub>3g</sub> )	$\Gamma_1$ $(A_e)$	6
	— Γ <sub>4</sub> (B <sub>3g</sub> ) —	$Z_1 (A_g)$	6
	$\Gamma_2$ $(B_{2g})$		7
$Z_2^ (B_{2g})$ —	$\Gamma_3$ (B <sub>1g</sub> ) $\Gamma_3$	$Z_2^+$ (B <sub>g</sub> )	7
$\Gamma_3^-$ (B <sub>1g</sub> ) —		$\Gamma_2$ (B <sub>e</sub> )	5
$Z_3^+$ (B <sub>1g</sub> )	$\Gamma_{2}^{+}(B_{2e})$	$Z_2^-(B_g)$	5

monoclinic phase  $(P2_1/b)$ . Table 3 shows that there is very good agreement in the observed frequencies for EACdC and MACdC. Additionally, the frequency shifts upon deuteration are very similar in the two compounds, other than for the mode at 144 cm<sup>-1</sup> in MACdC attributed to the CH<sub>3</sub> torsion of the methylammonium group. In EACdC, the CH<sub>3</sub> torsional mode is purely internal (see § 4). We conclude thus that the structure of EACdC below 114 K is monoclinic with space group  $P2_1/b$ .

In his independent study, Mokhlisse (1983) noted equally the similarity of the low-temperature Raman spectra of MACdC and EACdC and suggested the same space group for both crystals in their monoclinic phase.

**Table 3.** Raman frequencies (expressed in cm $^{-1}$ ) of the external modes of  $A_g$  symmetry in the MLT phase for MACdC and EACdC as well as their deuterated analogues. The  $d_3[I]$  analogues correspond to the CD $_3$ -substituted species, and those labelled  $d_3[II]$  to the ND $_3$  analogues. The values for MACdC and its analogues are taken from Mokhlisse *et al* (1983a). The symmetry coordinates refer to Geick and Strobel (1977). Parts of their tables are collected in the Appendix (table A1).

MACdC 20 K	EACdC 10 K	MA-d <sub>3</sub> (I) 20 K	EA-d <sub>3</sub> (I) 10 K	MA-d <sub>3</sub> (II) 20 K	EA-d <sub>3</sub> (II) 10 K	Assignment
51	50	51	48	51	50	Inorganic layer
66	61	62	57	67	60	External organic $(U_{33})$
72	71	68	72	72	72	Inorganic layer
93	90	90	84	93	90	Inorganic layer $(U_{57}-U_{96})$
106	99	99	95	102	98	External organic
112	123	112	121	109	122	Cl-M-Cl bending $(U_{57} + U_{96})$
130	113	130	113	123	111	$TV_z RNH_3(U_{27})$
144	105	108	100	132	102	External organic
160	151	155	146	153	143	External organic
164	157	160	157		156	Inorganic layer
187	178	187	175	180	171	External organic ( $U_{68}$ )
220	213	220	211	215	212	M-Cl stretching $(U_{51})$

#### 4. Assignment of the external modes

As can be seen in table 2, the six modes of  $A_g$  symmetry in the ORT phase at the centre of the Brillouin zone remain in the zone centre in all the three crystal phases. Three of

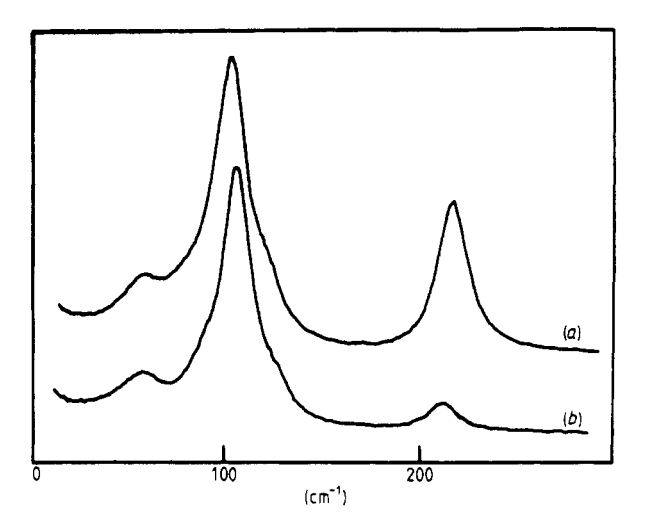
**Table 4.** Raman frequencies (expressed in cm. <sup>1</sup>) of the external modes of A, symmetry in the ORT phase (at 300 K) for the crystals MACdC, EAMC, PAMC (M =

Mn and (1977)	Mn and Cd). The values for N (1977) (see the Appendix).	es for MACdC Jix).	and its iso	topic analogue	s are taken fr	om Mokhlisse <i>et</i>	al (1983b). Th	e symmetry coo	Annual Cd). The values for MACdC and its isotopic analogues are taken from Mokhlisse et al (1983b). The symmetry coordinates refer to Geick and Strobel 1977) (see the Appendix).
	MACdC			EACdC					
$\mathbf{q}_0$	$d_3(I)$	$d_3(II)$	$\mathbf{q}_0$	$d_3(I)$	$d_3(II)$	EAMnC	PACdC	PAMnC	Assignment
65	09	65	59	52	09	57	47	47	$TV,A^+(U_n)$
<b>0</b> 8	08	08	84	08		16	77	81	$RV \overset{\circ}{CdCl}_{G} \overset{\circ}{(U_{ST}} - U_{sh})$
114	110	110	122	118	114	123	114	116	$M-CI$ 'bending' $(U_{c7} + U_{o6})$
128	123	123	103	66	66	106	93	46	$TVA^+(U_{27})$
172	173	163	164	159	159	161	186	184	$RVA^+(U_{cx}^{cx})$
213	213	212	214	213	215	212	212	206	$M-Cl$ 'stretching' ( $U_{s_1}$ )

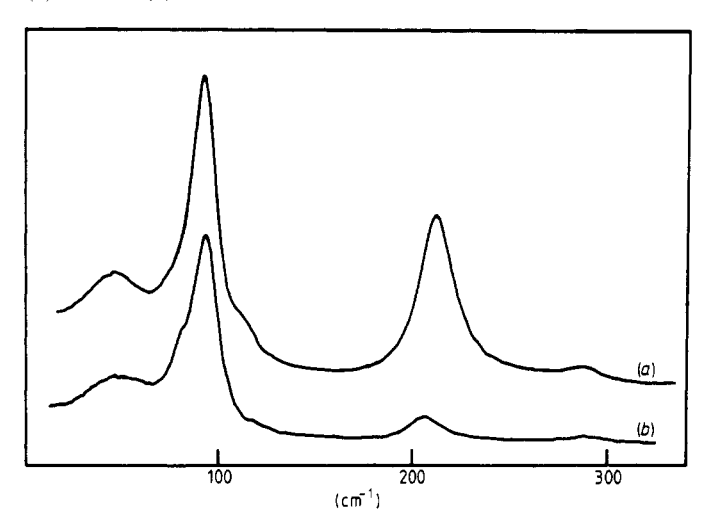
these modes pertain to motions of the inorganic layers, while the three remaining ones correspond to one librational and two translational modes of the alkylammonium group (Geick and Strobel 1977).

Table 4 collects the observed Raman frequencies in MACdC (Mokhlisse *et al* 1983b), EAMC and the propylammonium crystals PAMC (M = Mn and Cd). It appears that the spectra of these crystals are very similar (see figures 1 and 2) and the data can easily be correlated. The highest-frequency mode (observed at 214 cm<sup>-1</sup> in EACdC) is assigned to the metal–chlorine (axial) stretching mode. This assignment is supported by the following facts.

- (i) The frequency of this mode remains almost constant in the different crystals.
- (ii) As can be seen in figures 1 and 2, the relative intensity of this line depends on the metal (manganese or cadmium) contained in the crystal.



**Figure 1.** Polarised Raman spectra in the (cc) plane of EAMC crystals at room temperature. (a) M = Cd, (b) M = Mn.



**Figure 2.** Polarised Raman spectra in the (cc) plane of the propylammonium crystals PAMC at room temperature. (a) M = Cd, (b) M = Mn.

(iii) The linewidth of this mode as a function of temperature (see figure 3) is not significantly affected by the structural phase transition, while the external organic modes may exhibit significant broadening (Hagemann and Bill 1982b).

Figure 3 also shows the variation of the linewidth, as a function of temperature, of the mode found around 120 cm<sup>-1</sup>. The similarity of the behaviour of this mode to the behaviour of the stretching mode leads us to assign this mode to the Cl-M-Cl bending

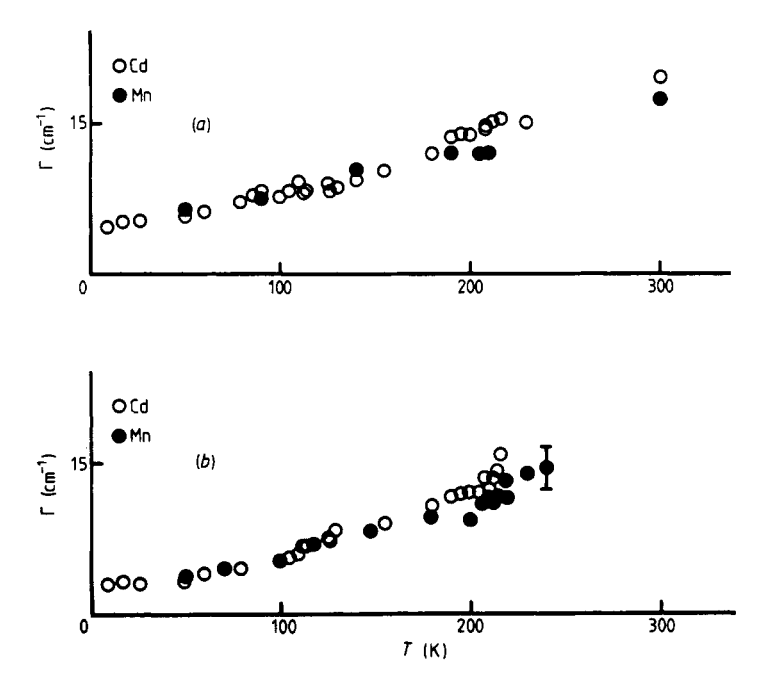


Figure 3. The observed Raman linewidth (FWHM), as a function of temperature, of the M-Cl stretching mode at around  $215 \text{ cm}^{-1}$  (a) and of the Cl-M-Cl bending mode observed around  $120 \text{ cm}^{-1}$  (b) in the crystals EAMC (M = Mn,Cd).

vibration. The frequency of the mode found around  $80\,\mathrm{cm}^{-1}$  does not change significantly for different crystals and is assigned to the third mode of  $A_g$  symmetry expected for the inorganic layers. Thus the three remaining modes are external organic modes.

The modes found at 128, 103 and 98 cm $^{-1}$  in MACdC, EACdC and PACdC, respectively, are assigned to the translatory modes along the z axis of the alkylammonium group. Indeed, the observed frequencies can be correlated with the inverses of the square roots of the masses of the organic moieties. Similarly, the lowest-frequency mode is assigned to the translatory mode along the x axis.

Finally, the remaining band is assigned to the librational mode. In EACdC, we have found a significant temperature dependence of the frequency of this mode (178 cm<sup>-1</sup> at 10 K, 164 cm<sup>-1</sup> at 300 K). We assume that the librational modes are more sensitive to the structural phase transitions, as we have observed around the MLT-OLT transition a very similar evolution of the NH<sub>3</sub> torsional mode and of an external mode assigned to another libration in EACdC (Hagemann and Bill 1982b).

The high frequency found for this mode in the propylammonium crystals requires

further investigation. We tentatively explain this observation by assuming a different type of coupling between vibrational states caused by the structural difference of the propylammonium crystal as compared with the other crystals investigated. Indeed, the difference between the lattice parameters a and b is significantly larger in the propylammonium crystals (0.221 and 0.23 Å in PAMnC and PACdC) than in the ethylammonium crystals (0.094 and 0.09 Å in EAMnC and EACdC). Depmeier (1979) has qualitatively discussed the uniqueness of the PAMnC crystal in the family of manganese crystals up to the decylammonium compound.

In the OLT phase we observe five out of six predicted additional modes of  $A_g$  symmetry in EACdC. Their frequencies are collected in table 5. The isotopic substitutions allow us to assign the lines found at 46, 68 and 156 cm<sup>-1</sup> to external modes of the inorganic layers.

The band observed at  $141 \, \mathrm{cm^{-1}}$  corresponds very probably to a librational mode of the ethylammonium group. We observe at the same frequency a mode of  $B_{3g}$  symmetry which we have assigned previously (Hagemann and Bill 1982b) to a librational mode.

								Assignment
Temperature (K)	10	155	155	155	10	140	300	
Phase	MLT	OLT	OLT	OLT	MLT	OLT	ORT	
Symmetry	$\mathbf{B}_{g}$	$\mathbf{B}_{1g}$	$B_{2g} \\$	$B_{3g} \\$	$\mathbf{A}_{g}$	$A_{g}$	$A_{g}$	
	_	48	46	47	50	46	_	Inorganic layer
	_	56	_	52	61	58	59	Ext. organic (TV)
	65	68	71	68	71	68	_	Inorganic layer
	83	83	84	85	90	86	84	Inorganic layer
	93	101	98	100	99	98	_	Ext. organic
	109		108	108	105	_	_	Ext. organic
	117	115	_	_	113	110	103	TV, RNH;
	_	124	124	124	123	124	122	Cd-Cl 'bending'
	166	160	_	136	151	141		Ext. organic
	137	138	136	154	157	156		Inorganic layer
	182	176	177	176	178	176	164	Ext. organic (RV)
		215	215	215	213	214	214	Cd-Cl 'stretching'

**Table 5.** Recapitulation and assignment of the external modes observed in the Raman spectra of EACdC in the different crystal phases.

Mokhlisse  $et\,al$  (1982) have assigned the  $A_g$  line at 141 cm $^{-1}$  to the torsional mode of the methyl group. We do not agree with this assignment for the following reasons. We have identified unambiguously the methyl torsional mode in EtNH<sub>3</sub>Cl at 290 cm $^{-1}$  (Hagemann and Bill 1984). In the OLT phase of EACdC, we observe in the (ca) and (cb) planes of polarisation one band at, respectively, 260 and 259 cm $^{-1}$ , which is not observed in the CD<sub>3</sub>-substituted crystal EACdC-d<sub>3</sub>[I]. In the same frequency region, these bands appear in the spectra of EAMnC in the OLT phase (figure 4). We assign these bands around 260 cm $^{-1}$  to the methyl torsional mode in the crystals EACdC and EAMnC.

The factor group analysis for the OLT phase shows that the 48 Raman-active external vibrations are evenly distributed over the four irreducible representations  $A_g$ ,  $B_{1g}$ ,  $B_{2g}$  and  $B_{3g}$ . For instance, the RV<sub>z</sub> libration of the organic group has four Raman-active

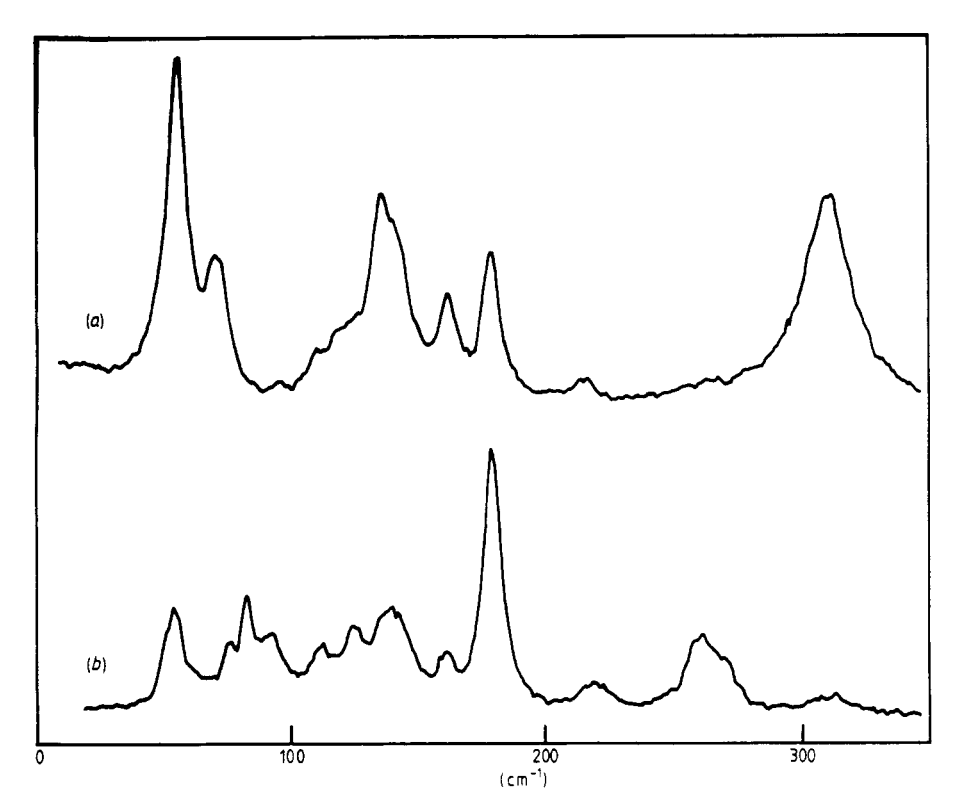


**Figure 4.** Raman spectra of EAMnC in the OLT phase at 80 K. (a) Symmetry of the polarisation:  $A_g + B_{1g}$ . (b) Symmetry of the polarisation:  $B_{2g} + B_{3g}$ .

components, one for each Raman-active irreducible representation. Accordingly, we can expect similar frequencies in the different planes of polarisation for a given type of motion of the organic group. This is generally observed, as can be seen in table 5. The assignments proposed for the  $A_g$  modes are transferred by analogy to the  $B_{ng}$  modes. These assignments are additionally supported by our isotopic substitutions.

However, two modes in table 5 do not follow the scheme outlined above. The corresponding lines are found at 137 and 166 cm $^{-1}$  in the  $B_g$  spectra at 10 K. The 137 cm $^{-1}$  band corresponds very probably to a deformation of the inorganic layer other than the related  $A_g$  mode. The frequency of 166 cm $^{-1}$  is not too far from the corresponding value found for the  $A_g$  symmetry (151 cm $^{-1}$ ) at 10 K. Table 5 shows that the  $A_g$ -active mode changes considerably with increasing temperature, while the  $B_g$ -active mode is much less sensitive. Additionally, the frequency shift of the 151 cm $^{-1}$  line upon deuteration of the NH $_3$  group is more important than the shift of the 166 cm $^{-1}$  line. These shifts are of 8 and 4 cm $^{-1}$  respectively (Hagemann and Bill 1982a). These observations suggest the presence of different vibrational couplings between internal and external modes in the different symmetries for these two lines.

#### 5. The MLT-OLT transition in EACdC

We have shown that the space group of EACdC in the MLT phase is  $P2_1/b$ . This group

is a maximal subgroup of the OLT space group Pbca ('translationsgleich'). The second Landau criterion for a second-order transition is not satisfied, as can be seen in table 2. The zone-centre modes of the OLT phase are distributed evenly in zone-centre and zone-boundary modes in the MLT phase. Thus, there is no irreducible representation of the space group Pbca that becomes exclusively the unique totally symmetric representation of the group  $P2_1/b$ . It follows that the MLT-OLT transition is a first-order one (but this does not indicate how strongly it is of first order).

Experimentally, strong first-order character is observed in the sudden and marked change of the Raman spectra around this transition. Several of the observed changes have been described previously (Hagemann and Bill 1982b).

Figure 5 shows schematically (without indicating the monoclinicity) the projections

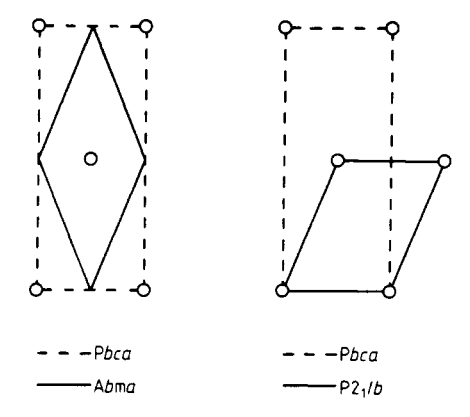


**Figure 5.** The projection of the elementary cell in the bc plane (only the cadmium atoms are shown) in the three crystal phases of EACdC. The monoclinic displacement of the P2<sub>1</sub>/b phase is not indicated in the figure.

of the bc face of the primitive cell in the different crystal phases. The experimental results indicate that the monoclinic deformation lies in the bc plane. Consequently, the unique twofold axis (along a) lies in the plane of the inorganic layer. We have suggested on the basis of measurements of linewidth as a function of temperature (Hagemann and Bill 1982b) that this transition is related to torsional and librational motions of the organic group, associated with a small distortion of the lattice.

This set of experimental results and group theoretical considerations shows that the MLT-OLT transition is a first-order displacive phase transition triggered by the degrees of freedom of motion of the ethylammonium group.

#### 6. The OLT-ORT transition in EACdC and EAMnC

The group theoretical analysis by Geick and Strobel (1977) shows that Pbca is a maximal subgroup of Abma and that the second Landau criterion is also satisfied.

We now suggest a method for defining the order parameter associated with this phase transition. The ethylammonium groups are located on two sites placed symmetrically

on opposite sides of the crystallographic mirror [m] in the disordered phase Abma. At high temperatures  $(T > T_{\rm c})$  the probability of occupation of one site or the other by the organic group is  $p_1 = p_2 = 0.5$ . At  $T < T_{\rm c}$  these probabilities become  $p_1(p_2) = 1$  and  $p_2(p_1) = 0$ . The crystal is ordered. The order parameter may then be written as

$$\eta = n(p_1 - p_2)$$

and expresses the difference of population of the equilibrium positions that can be occupied by the ethylammonium group. At  $T = T_c$ ,  $\eta = 0$ .

The free energy associated to this phase transition takes the form (Toledano and Toledano 1982)

$$F = \frac{1}{2}a\eta^2 + \frac{1}{2}b\eta^4 + \dots$$

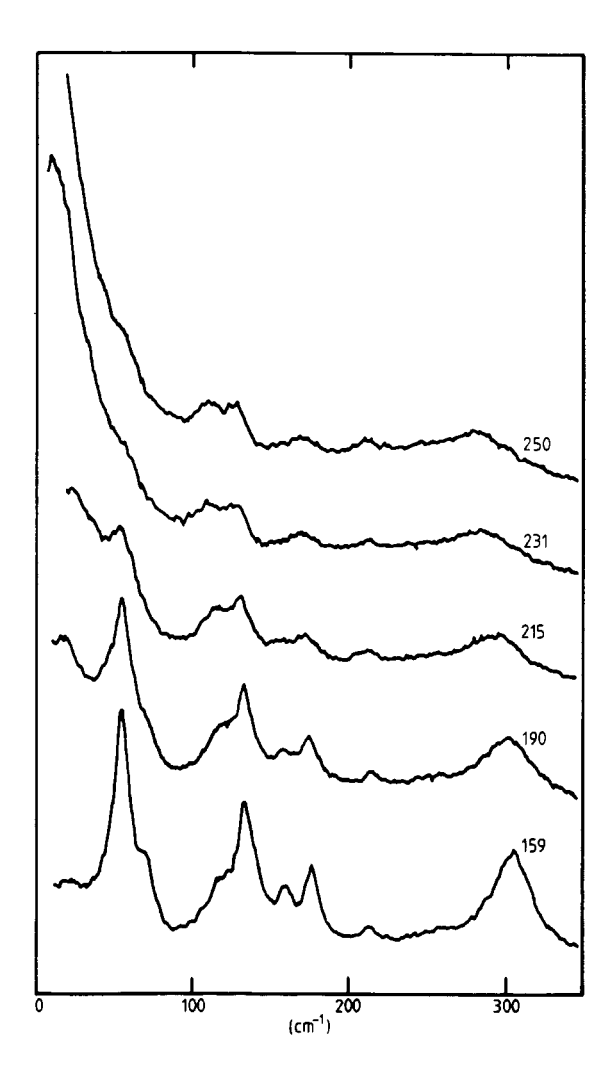


Figure 6. Polarised Raman spectra  $(A_g + B_{1g})$  of EAMnC around the OLT-ORT phase transition, at various temperatures given by spectra in K.

For a second-order transition, the Landau theory requires that the coefficient b is positive.

The experimental investigations performed on EACdC using optical inspection (Chapuis 1977), dielectric (Levstik and Filipic 1980) and specific heat (Tello *et al* 1977) measurements all show a thermal hysteresis of 1 K. This hysteresis suggests that the coefficient *b* is negative. The phase transition is therefore slightly of first order.

The dielectric measurements performed on EAMnC (Filipic and Levstik 1980) revealed no thermal hysteresis. A thorough investigation of the birefringence (Käräjämäki *et al* 1981) showed equally no thermal hysteresis at this phase transition. An independent birefringence study (Brunskill and Depmeier 1982) of the same crystal showed, however, a small hysteresis of 0.4 K at the OLT-ORT transition.

Our experimental low-frequency Raman spectra of EACdC and EAMnC around this phase transition are very similar and exhibit a quasi-continuous behaviour (see figure 6). The dynamics associated with this transition manifests itself, however, clearly in the increase of the observed linewidth and in the presence of a large Rayleigh wing in the disordered phase. The modes that exhibit the largest increases of linewidth at the phase transition are the internal modes related to the NH<sub>3</sub> group. Among these, the NH<sub>3</sub> torsional mode exhibits additional properties. In the disordered ORT phase it is observed in the (aa), (bb) and (ab) planes, the same planes of polarisation in which the Rayleigh wings appear. Figure 7 shows the observed variation of the linewidth and line position

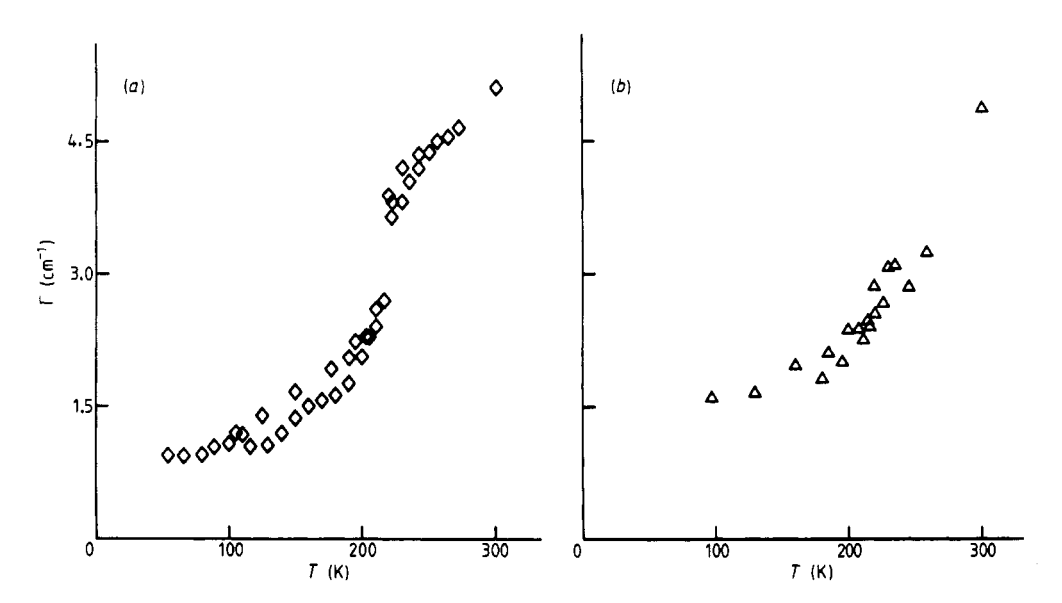


Figure 7. The Raman linewidth as a function of temperature of the C-C stretching mode (observed around  $870 \,\mathrm{cm}^{-1}$ ) in EAMC for (a) M = Cd and (b) M = Mn.

of this mode in EACdC and EAMnC. We can see that its line position jumps at the transition temperature towards lower frequencies with increasing temperature. The evolution of the linewidth is more difficult to describe, as the lineshape at high temperatures is no longer symmetrical (see figure 6). This complex behaviour suggests that the NH<sub>3</sub> torsional mode is subject to rather strong anharmonic coupling with a mode related to the order parameter.

Mokhlisse etal(1982) have associated the Rayleigh wing and the  $NH_3$  torsional mode observed in the ORT phase in EACdC with the dynamic properties of the crystal. They assigned the Rayleigh wings to an overdamped rocking motion of the  $CdCl_6$  octahedra occurring in the time between the reorientation steps of the ethylammonium group. This assignment is supported by a group theoretical analysis of the  $CdCl_6$  rocking motion which accounts for the observed polarisations.

This rocking mode is coupled to the reorientational motion of the organic group through hydrogen bonding interactions. The reorientational frequency of the ethylammonium group is expected to be in the microwave range  $(10^9-10^{11}\,\mathrm{s}^{-1})$ , depending on temperature), by analogy with the experimental estimates for the methylammonium group in MACdC (Mokhlisse *et al* 1982).

Brillouin scattering experiments on EAMnC have been published (Käräjämäki *et al* 1981). They show that the crystal is ferroelastic at low temperatures in a conventional classification.

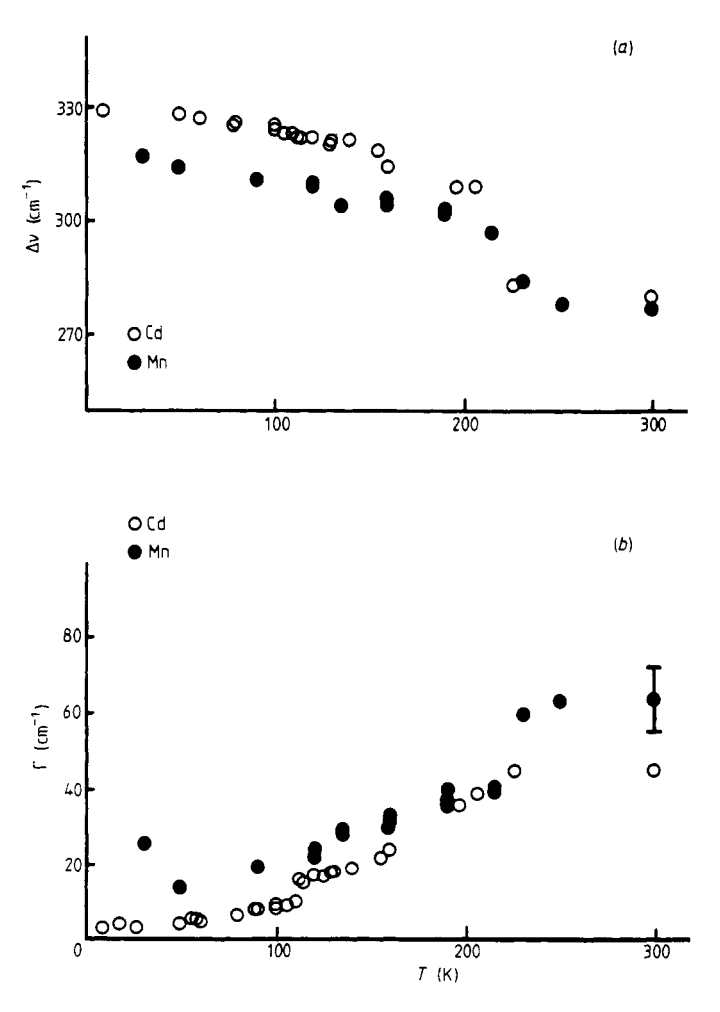


Figure 8. An illustration of the behaviour of the  $NH_3$  torsional mode as a function of temperature in the crystals EAMC (M = Cd and Mn). (a) Line position as a function of temperature. (b) Linewidth (FWHM) as a function of temperature.

Combining the considerations and results mentioned above, we may postulate tentatively a coupled anharmonic motion of the reorientation coordinate of the organic group (the pseudo-spin coordinate), the hydrogen bond coordinate and the pseudo-rotation of the MCl<sub>6</sub> octahedra. The question of whether these can be considered as entities that are mutually perturbed or whether they all perform a common coherent motion remains unanswered.

The NH<sub>3</sub> torsional mode is very sensitive to variations in strength of hydrogen bonding. It is probably through this coupling that it is so strongly affected by the above-mentioned movements. This postulate must be further analysed by theoretical and experimental investigations, namely by Brillouin scattering and ENDOR experiments and by a theoretical analysis of the experimental spectra. This work is, however, beyond the scope of the present paper. An ENDOR study on manganese-doped EACdC is under way.

In order to investigate the effect of the disorder on internal vibrations not related to the NH<sub>3</sub> group, we have measured the variation of linewidth as a function of temperature of the C–C stretching mode found around 870 cm<sup>-1</sup>. The results for EACdC and EAMnC are presented in figure 7. At low temperatures, the linewidth (FWHM) is found to be very small (about 0.9 cm<sup>-1</sup> at 54 K in EACdC). This line is much sharper than the lines pertaining to the external modes observed at the same temperature. Figure 7 shows that at the OLT-ORT transition, the linewidth jumps in EACdC, while no discontinuous behaviour appears in EAMnC.

We have mentioned above that in EACdC a thermal hysteresis of 1 K was observed using various experimental techniques, while in EAMnC this hysteresis appeared to be much smaller or non-existent. This linewidth measurement of the C–C stretching mode indicates that the OLT-ORT transition in EAMnC might have second-order character. Indeed, the Raman linewidths are strongly dependent on the fluctuations of the order parameter. These latter ones are in general important in a first-order transition and rather continuous in a second-order one. The linewidth measurement of the NH $_3$  mode (figure 8) shows similarly a smoother behaviour for EAMnC at the OLT-ORT transition, but the experimental results are less precise. It is useful here to recall the observation that much less twinning is induced by thermal cycling through the OLT-ORT transition in EAMnC crystals than in crystals of EACdC.

This different behaviour of the linewidth is the only fundamental difference that we have observed in comparing the OLT-ORT transition in EACdC and EAMnC. Nevertheless, our present results do not allow us to conclude that this transition is definitely a second-order transition in EAMnC. However, we think that the experimental measurement of Raman linewidth is a very sensitive probe of dynamical processes related to structural phase transitions.

#### 7. Conclusion

The space group of EACdC below 112 K has been shown to be  $P2_1/b$  by isotopic substitution as well as by Raman measurements where polarisation and temperature varied.

The MLT-OLT transition in EACdC appears to be a first-order displacive phase transition.

The external vibrations in the three crystal phases have been assigned. The proposed

assignments are complicated by some superpositions of vibrational couplings between internal and external modes which need further investigation.

Crystals of the family  $(RNH_3)_2MCl_4$  with R = methyl, ethyl, propyl and M = Mn and Cd exhibit similar Raman spectra in the same crystal phase, as shown in the MLT (table 3) and in the ORT (table 4) phase.

The anharmonic couplings due to the dynamic disorder in the ORT phase need further experimental and theoretical investigation.

## Acknowledgment

We thank J L Clignez and F Rouge for technical assistance during this investigation. This work was supported by the Swiss National Science Foundation.

## **Appendix**

In this Appendix we recall the symmetry coordinates of the  $A_g$  modes obtained by Geick and Strobel (1977). They are collected in table A1. In this table,  $u_{m\alpha}$  means a translational motion of particle m (identified in figure A1) in the  $\alpha$  direction. The librational motions of particle m around the  $\beta$  axis are labelled  $s_{m\beta}$ .

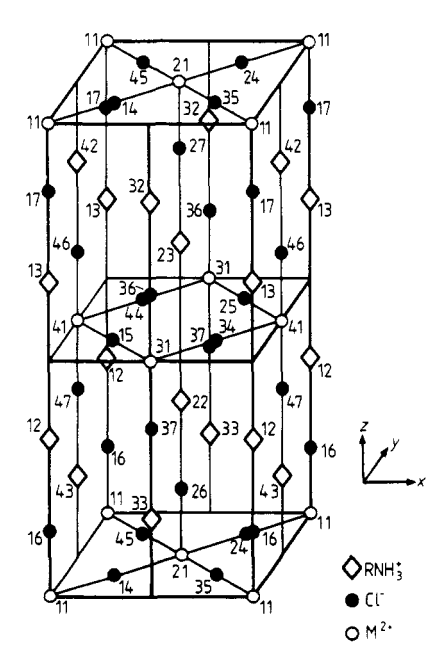


Figure A1. A schematic representation of the unit cell of EAMC crystals. The labels of the rigid particles refer to the symmetry coordinates in table A1. A drawing showing in detail the position of the  $C_2H_5NH_3$  in its local environment is given, for instance, by Chapuis (1977).

**Table A1.** Symmetry coordinates of the external modes of  $A_g$  symmetry in the crystals EAMC obtained by Geick and Strobel (1977).

Modes expected at the centre of the Brillouin zone, just for the OLT (Pbca) phase

```
\begin{array}{l} U_{29} = N \left(u_{12}, -u_{13}, +u_{22}, -u_{23}, -u_{32}, +u_{33}, -u_{42}, +u_{43}\right) \\ U_{53} = N \left(u_{16}, -u_{17}, +u_{26}, -u_{27}, -u_{36}, +u_{37}, -u_{46}, +u_{47}\right) \\ U_{64} = N \left(s_{12}, +s_{13}, +s_{22}, +s_{23}, -s_{32}, -s_{33}, -s_{42}, -s_{43}\right) \\ U_{74} = N \left(s_{12}, +s_{13}, -s_{22}, -s_{23}, +s_{32}, +s_{33}, -s_{42}, -s_{43}\right) \\ U_{91} = N \left(u_{14}, +u_{15}, -u_{24}, -u_{25}, +u_{34}, +u_{35}, -u_{44}, -u_{45}\right) \\ U_{104} = N \left(u_{14}, -u_{15}, -u_{24}, +u_{25}, +u_{34}, -u_{35}, -u_{44}, +u_{45}\right) \end{array}
```

Modes expected at the centre of the Brillouin zone for the ORT, OLT and MLT phases

```
\begin{array}{l} U_{27} = N \left( u_{12z} - u_{13z} + u_{22z} - u_{23z} + u_{32z} - u_{33z} + u_{42z} - u_{43z} \right) \\ U_{33} = N \left( u_{12x} - u_{13x} - u_{22x} + u_{23x} - u_{32x} + u_{33x} + u_{42x} - u_{43x} \right) \\ U_{51} = N \left( u_{16z} - u_{17z} + u_{26z} - u_{27z} + u_{36z} - u_{37z} + u_{46z} - u_{47z} \right) \\ U_{57} = N \left( u_{16x} - u_{17x} - u_{26x} + u_{27x} - u_{36x} + u_{37x} + u_{46x} - u_{47x} \right) \\ U_{68} = N \left( s_{12y} + s_{13y} - s_{22y} - s_{23y} - s_{32y} - s_{33y} + s_{42y} + s_{43y} \right) \\ U_{96} = N \left( u_{14z} + u_{15z} - u_{24z} - u_{25z} - u_{34z} - u_{35z} + u_{44z} + u_{45z} \right) \end{array}
```

#### References

Blinc R, Burgar M, Lozar B, Seliger J, Slak J, Rutar V, Arend H and Kind R 1977 J. Chem. Phys. 66 278 Brunskill I H and Depmeier W 1982 Acta Crystallogr. A 38 132

Chapuis G 1977 Phys. Status Solidi a 43 203

Depmeier W 1977 Acta Crystallogr. B 33 3713

— 1979 J. Solid State Chem. 29 15

Depmeier W and Heger G 1978 Acta Crystallogr. B 34 1698

Filipic C and Levstik A 1980 Phys. Status Solidi a 57 K55

Geick R and Strobel K 1977 J. Phys. C: Solid State Phys. 10 4221

Hagemann H 1984 PhD Thesis University of Geneva

Hagemann H and Bill H 1982a Chem. Phys. Lett. 87 45

— 1982b Chem. Phys. Lett. 93 582

— 1984 J. Chem. Phys. 80 111

Käräjämäki E, Laiho R, Levola T, Kleemann W and Schäfer F J 1981 Physica B 111 24

Kind R 1980 Ferroelectrics 24 81

Levstik A and Filipic C 1980 Phys. Status Solidi a 58 K165

Mokhlisse R 1983 Thèse d'Etat University of Bordeaux

Mokhlisse R, Couzi M and Lassegues J C 1983a J. Phys. C: Solid State Phys. 16 1353

Mokhlisse R, Couzi M and Loyzance P L 1983b J. Phys. C: Solid State Phys. 16 1367

Mokhlisse R, Couzi M and Wang C H 1982 J. Chem. Phys. 77 1138

Oxton I A 1979 J. Mol. Struct. 54 11

Peyrard M and Perret R 1979 Phys. Status Solidi a 52 521

Rehaber E 1976 Diploma thesis University of Regensburg

Stoelinga J H M and Wyder P 1974 J. Chem. Phys. 61 478

Tello M J, Arriandiaga M A and Fernandez J 1977 Solid State Commun. 24 299

Toledano P and Toledano J C 1982 Phys. Rev. B 25 1946